

Supplemental Materials and Methods:

Chemicals were obtained from Sigma-Aldrich, unless specified otherwise. Satavaptan was kindly provided by Sanofi-Aventis (Toulouse, France) while tolvaptan was a gift from Ostuka Pharmaceutical (Tokyo, Japan).

Clinical Data

This is a retrospective review of the clinical phenotypes of a single individual affected with nephrogenic syndrome of inappropriate antidiuresis cared for by the authors.

Constructs, Cell Culture and Transfections

Expression plasmids coding for the wild-type myc-tagged V2R used in this study was previously described.¹ The myc-F229V-V2R, myc-R137C-V2R and myc-R137L-V2R were generated using the *Quick Change* mutation kit (Agilent Technologies, Santa-Clara, USA) using the manufacturer's protocol. YFP-tagged versions of the WT-, R137C- and R137L-receptors were previously described² while the F229V-V2R-YFP plasmid was generated from WT-V2R-YFP using the *Quick Change* mutation kit. The functionality of the YFP- and myc-tagged receptors was validated by radioligand binding and cAMP production assay. No difference in AVP binding affinity or potency to promote cAMP production were observed between the tagged and untagged wild-type receptors (see supplemental Table 1). The β -arrestin2-Rluc² and the dominant negative mutant of Dynamine2 (K44A)³ were also described. HEK293T or HEK293T/AP2-YFP³ cells were maintained in Dulbecco's modified Eagles's medium (DMEM; Wisent Bioproducts, Qc, Canada) supplemented with 10% fetal bovine serum (Wisent Bioproducts) in a 37°C humidified incubator with 5% CO₂ atmosphere. Transfections were performed using Lipofectamine 2000 (Invitrogen, Grand Island, NY) according to the manufacturer's recommendations.

Confocal microscopy

HEK293T cells transfected with the YFP-tagged version of the different receptors studied were seeded on poly-D-lysine-coated glass bottom petri dishes (MatTek Corporation, Ashland MA) and fixed with paraformaldehyde prior to their observation under a Zeiss LSM 510 Laser Scanning Confocal Microscope (Jena, Germany) equipped with a 100x plan-Apo NA 1.4, DICIII objective and a 505 nm long pass emission filter. Excitation was performed with a 488 nm laser. Image acquisitions were performed with the LSM 510 Software, version 3.2, service pack 2.

Western blotting

Transiently transfected cells were lysed in lysis buffer (50 mM HEPES, 150 mM NaCl, 1% Triton X-100, 0.5% Na-deoxycholate, 1 mM PMSF) 48 hours post-transfection. Western blotting and SDS-PAGE were performed using standard protocols with the 9E10 anti-myc antibody (Santa-Cruz Biotechnology, CA) followed by an HRP-conjugated goat anti-mouse secondary antibody (GE healthcare, UK). Westerns were revealed using the Western LightningTM chemiluminescence substrate (Perkin Elmer, MA) and the LAS-3000 Imaging System (Fuji, Japan). Band quantifications were done using the Multi Gauge quantification software (Fuji). The level of exposure shown was chosen to allow the visualization of the mature form of the receptor, even for the poorly mature mutant forms of the receptor. The quantification was realized using exposures that remained within the linear range of quantification of the system and the data expressed as the ratio of mature/immature forms of the receptor. For each region quantified, the luminescence signal was averaged as a function of the size of the area and the corresponding background subtracted.

Cell surface ELISA.

Cell surface receptor expression was assessed as described previously.² Briefly, HEK293T cells were seeded in 6-well plates (4×10^5 cells/well) and transfected with the indicated receptors constructs the next day. 48h following transfection, cells were fixed with Tris-buffered saline (TBS; 10 mM Tris, 150 mM NaCl,

pH7.4) containing 3.7% formaldehyde for 5 min at room temperature, washed with TBS and blocked with 1% BSA-containing TBS (TBS-B). The blocking buffer was then replaced with the 9E10 mouse monoclonal anti-myc antibody diluted in TBS-B, washed again and incubated with an alkaline phosphatase-conjugated anti-mouse antibody (BIO-RAD). After washing, cell surface expression was determined by the colorimetric reaction initiated by the addition of the *Alkaline phosphatase conjugate substrate kit* (BIO-RAD) which was stopped by adding NaOH to the wells. The intensity of the reaction was quantified using a OASYS UVM340 microplate spectrophotometer (Montreal Biotech inc. Montreal, Canada) at 405 nm. Net surface expression was determined by subtracting the absorbance values obtained with the mock transfected wells. All the results were generated in triplicates.

cAMP measurements

cAMP measurements were performed using either a CRE-luciferase gene reporter assay or the EPAC-BRET biosensor as described below. For the CRE-luciferase assay, HEK293T cells were transfected with the corresponding myc-tagged receptor construct along with the pCRE-Luc vector purchased from Clontech (Mountain View, CA) and the pRL-CMV plasmid (Promega Corporation, Madison, WI). Three hours after transfection, cells were exposed to satavaptan, tolvaptan or vehicle and incubated for 16 hours at 37°C. Cells were then lysed in lysis buffer, and 10 µL of the lysates were distributed in a white opaque 96-well plate (Perkin Elmer, Waltham, MA). Luciferase activities were measured using the Veritas luminometer from Promega by injecting the Firefly luciferase substrate (D-luciferin, Biotium, Hayward, CA) or the *Renilla* luciferase substrate (Coelenterazin h, Prolume, Pinetop, AZ). Luminescent values obtained with the Firefly luciferase substrate (pCRE-Luc) were divided by the values obtained with the *Renilla* luciferase substrate (pRL-CMV) for normalization. For the EPAC-BRET biosensor, the myc-tagged WT-V2R or F229V-V2R were transfected in HEK293T cells along with the previously described biosensor construct.⁴ Following a 48-h incubation at 37°C, cells were transferred into 96-well plates at a density of 8 to 10x10⁴ cells per well in PBS. Vehicle, satavaptan (10 µM), tolvaptan (10 µM) or AVP (1 µM) were added along with the luciferase substrate DeepBlue C (Nanolight Technology, AZ, USA) and the plate was read repetitively for 20 min in a Mithras LB940 instrument (Berthold Technologies, Bad Wildbad,

Germany) using the MicroWin 2000 software (Berthold Technologies). For the dose-response curves, varying concentrations of either AVP or tolvaptan were added to the wells and the plate incubated at 37°C for 15 min prior to reading. The BRET signal is determined by calculating the ratio of the light emitted at 505-555 nm (YFP) over the light emitted at 465-505 nm (Luciferase). Experiments were performed in triplicates.

β-arrestin2/receptor and β-arrestin2/AP2 interactions

The interactions between β-arrestin2 and either V2R or AP2 were monitored by BRET, as previously described.² For β-arrestin2-*Rluc*/receptor interaction, YFP-tagged constructs (WT-V2R-YFP, F229V-V2R-YFP and R137C-V2R-YFP) were co-transfected with the β-arrestin2-*Rluc* construct in HEK293T cells. After 48 h, cells were transferred into 96-well plates at a density of 8 to 10x10⁴ cells per well in PBS and exposed (or not) to 1 μM AVP for 15 min prior to BRET reading. For β-arrestin2-*Rluc*/AP2-YFP interaction, HEK293T cells stably expressing the AP2-YFP construct³ were co-transfected with β-arrestin2-*Rluc* along with the indicated myc-tagged receptor construct, with or without the dominant negative Dynamin2 (DynK44A) construct.³ For both experiments, the *Rluc* substrate coelenterazin H (5 μM) was added 5 min prior to reading. BRET signal is determined by calculating the ratio of the light emitted at 505-555 nm (YFP) over the light emitted at 465-505 nm (Luciferase). Experiments were performed in triplicates.

Binding experiments

Radioligand binding experiments were performed on HEK293T or HEK293-AP2 cells transfected with plasmids encoding the specified receptor constructs. 24 h after transfection, cells were transferred into poly-D-lysine-coated 24-well culture plates. The next day, each well was first rinsed with ice-cold washing buffer (PBS containing 2% glucose and 1% BSA) prior to incubation of cells with increasing concentrations of [³H]arginin vasopressin (64.2 Ci/mMol, Perkin Elmer, MA, USA) for 2 hours in binding buffer (0.1% glucose, 1% BSA, 1mM tyrosine, 1mM phenylalanine in PBS) on ice. For cell surface

receptor number determination, a saturating concentration of [³H]arginin vasopressin (40 μM) was used. After the incubation period, the attached cells were washed three times with ice-cold washing buffer to remove unbound ligand. Cells were then lysed with 0.4 M NaOH. The radioactivity was determined by scintillation counting. Specific binding was determined by subtracting the counts obtained with the mock-transfected cells. Each data point was performed in triplicates.

Receptor modeling

To provide a structural basis for constitutive activation in AVPR2, we used a *de novo* structure prediction methodology called GEnSeMBLE (GPCR Ensemble of Structures in Membrane BiLayer Environment)⁵ to predict the most stable conformations for the wild-type (WT) receptor and two mutants (F229V and R137C). The methodology samples all possible seven transmembrane (TM) helix bundle conformations in the local conformational space of helix orientations in the membrane (~6 billion conformations in the current case for each of the three receptor forms) using a fast but efficient BiHelix procedure.⁶ This sampling procedure splits up the large 7-helix bundle conformational sampling into complete 2-helix conformational samplings involving nearest-neighbour helices, constructs the 7-helix bundle energies by adding up all the 2-helix energies appropriately, and ranks the resulting 7-helix conformations by energy. The top 2000 conformations (out of ~6 billion) are reranked using a more accurate energy by explicitly building the 7-helix bundles and optimizing the sidechains. The method has been used successfully to predict the structures of many GPCRs.^{7,8}

References:

1. Morello JP, Salahpour A, Laperriere A, Bernier V, Arthus MF, Lonergan M, Petaja-Repo U, Angers S, Morin D, Bichet DG, Bouvier M: Pharmacological chaperones rescue cell-surface expression and function of misfolded V2 vasopressin receptor mutants. *J Clin Invest* 105: 887-95, 2000
2. Rochdi MD, Vargas GA, Carpentier E, Oligny-Longpre G, Chen S, Kovoov A, Gitelman SE, Rosenthal SM, von Zastrow M, Bouvier M: Functional characterization of vasopressin type 2

receptor substitutions (R137H/C/L) leading to nephrogenic diabetes insipidus and nephrogenic syndrome of inappropriate antidiuresis: implications for treatments. *Mol Pharmacol* 77: 836-45, 2010

3. Hamdan FF, Rochdi MD, Breton B, Fessart D, Michaud DE, Charest PG, Laporte SA, Bouvier M: Unraveling G protein-coupled receptor endocytosis pathways using real-time monitoring of agonist-promoted interaction between beta-arrestins and AP-2. *J Biol Chem* 282: 29089-100, 2007
4. Breton B, Sauvageau E, Zhou J, Bonin H, Le Gouill C, Bouvier M: Multiplexing of multicolor bioluminescence resonance energy transfer. *Biophys J* 99: 4037-46, 2010
5. Abrol R, Griffith AR, Bray JK, Goddard WA, 3rd. Structure Prediction of G Protein-Coupled Receptors and Their Ensemble of Functionally Important Conformations. In: Vaidehi N, Klein-Seetharaman J, eds. *Methods in Molecular Biology 'Special issue on Membrane Protein Structure Predictions Methods: Methods and Protocols'*. New York: Humana; pp. 237-254, 2012
6. Abrol R, Bray JK, Goddard WA, 3rd: Bihelix: Towards de novo structure prediction of an ensemble of G-protein coupled receptor conformations. *Proteins* 80: 505-518, 2011
7. Kim SK, Riley L, Abrol R, Jacobson KA, Goddard WA, 3rd: Predicted structures of agonist and antagonist bound complexes of adenosine A3 receptor. *Proteins* 79: 1878-97, 2011
8. Kim SK, Fristrup P, Abrol R, Goddard WA, 3rd: Structure-based prediction of subtype selectivity of histamine H3 receptor selective antagonists in clinical trials. *Journal of chemical information and modeling* 51: 3262-74, 2011

Supplementary Table 1

Table S1: Effect of YFP and myc tags addition on the functionality of the WT-V2R. AVP dose-response curve were performed on HEK293T cells transfected with either the untagged, YFP-tagged or myc-tagged version of the WT-V2R to determine the EC₅₀ of cAMP production using the EPAC BRET biosensor. ³H-AVP saturation binding experiments were also performed to determine the affinity of AVP for the different receptor species. Experimental procedures for both experiments are described in the detailed method section.

Receptor	Log EC ₅₀ (M)	KD (nM)
Untagged	-9.67 +/- 0.12	20.4 +/- 1.92
Myc-tagged	-9.4 +/- 0.13	18.8 +/- 1.87
YFP-tagged	-9.416 +/- 0.15	18.33 +/- 1.55

Supplementary Figure 1

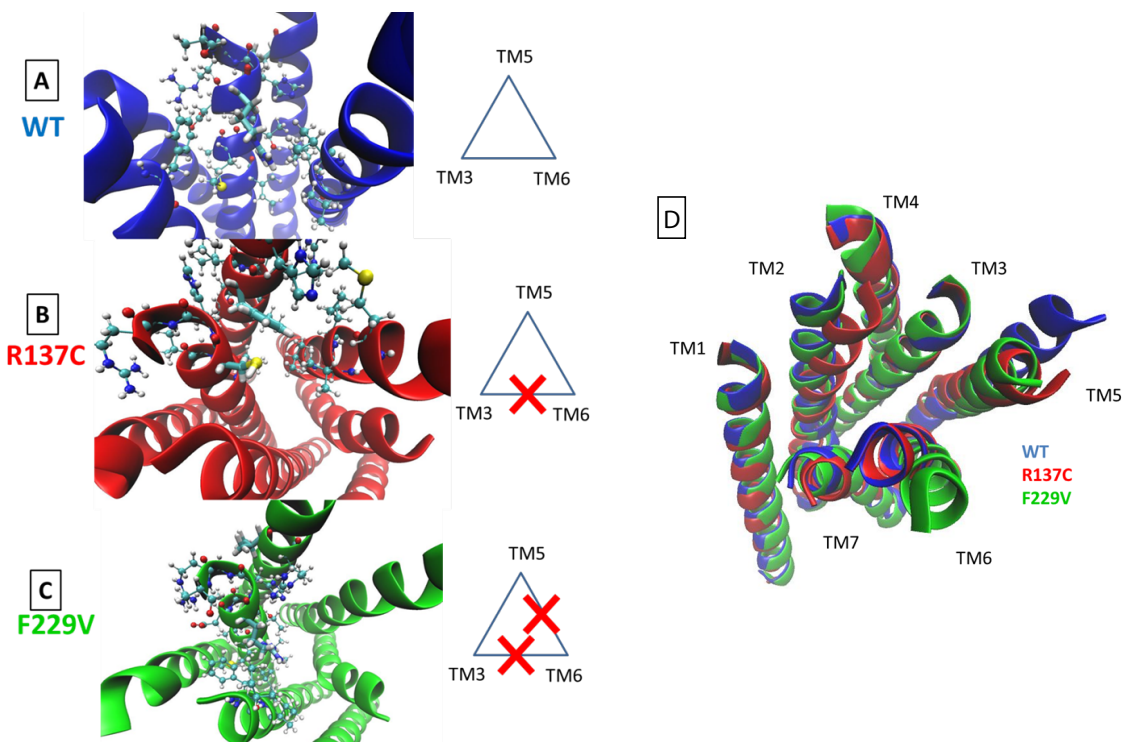


Figure S1: Cytoplasmic view of the lowest energy structure for the WT, R137C and F 229V-V2R. Residues 137 and 229 are shown in licorice representation; all others are shown in ball and stick representation. A) WT -V2R: The R137 (3.50) residue on TM3 forms an intra-helical hydrogen bond with T134. This arginine usually forms a salt bridge with Glu/Asp (6.30 residue) on the TM6 in many class A GPCRs, which is V266 in the AVPR2 receptor. Thus, the classical ionic lock believed to maintain GPCRs in their inactive state does not exist in the V2R. On the cytoplasmic side, TM3 is coupled to TMs 5 and 6 mainly through hydrophobic interactions. TMs 5 and 6 are linked through a hydrogen bond between T205 (TM5) and W296 (TM6). The interaction triangle on the right of Figure S1A shows the cytoplasmic facing coupling between TMs 3, 5, and 6. B) R137C: The cytoplasmic end of TM5 moves closer to TM6 (relative to WT) forming a polar interaction between H233 (TM5) and K268 (TM6). The lack of R137 leads to a cytoplasmic uncoupling of TM3-TM6 interaction as shown in the interaction triangle on the right of Figure S1B. This uncoupling is caused by an inward movement of TM2, as the salt bridge interaction between E40 on TM1 and K100 on TM2 seen in WT is lost in R137C mutant. C) F229V: The cytoplasmic end of TM6 moves away from TMs 3 and 5. The D136 residue, which forms an intra-helical interaction with R139 residue (one helix turn below D136) in the WT, R137C, and F229V structures, also forms an inter-helical salt bridge interaction with R158 (TM4). D) Superposed ribbon structures of WT-, R137C-, and F229V-V2R. The major movements that occur in the F229V involves TM6 getting uncoupled from both TM3 and TM5 whereas for R137C, the uncoupling of TM6 from TM3 is not sufficient to lead to a major movement of these helices. However a significant inward movement of TM2 is observed compared to both WT and F229V-V2R. Both R137C and F229V mutations result in an inward movement of TM5 compared to WT-V2R. The active structures of a few GPCRs have been crystallized and suggest that the motion of TM6 plays a major role in activation.¹ The predicted structures of the mutant AVPR2 receptors are consistent with this observation. In addition, the full uncoupling of TM6 from TM3 and TM5 and large outward movement of TM6 in the F229V mutant can potentially explain the high constitutive activity of the F229V mutant. The potential roles of the TM5 and TM2 movements in the constitutive activation profiles remain to be investigated, as is the role of slight outward movement of TM7 for R137C mutant in any beta-arrestin activity.

Reference:

1. Abrol R, Griffith AR, Bray JK, Goddard WA, 3rd: Characterizing and predicting the functional and conformational diversity of seven-transmembrane proteins. *Methods* 55: 405-414, 2011